

# Anisotropic Spherically Symmetric Collapsing Star From Higher Order Derivative Gravity Theory

HOSSEIN GHAFARNEJAD

Faculty of Physics, Semnan University, Semnan, IRAN, Zip code: 35131-19111\*

**ABSTRACT-** Adding linear combinations  $R^2$ ,  $R_{\mu\nu}R^{\mu\nu}$  and  $R_{\mu\nu\gamma\delta}R^{\mu\nu\gamma\delta}$  with Einstein-Hilbert action we obtain interior metric of an anisotropic spherically symmetric collapsing (ASSC) stellar cloud. We assume stress tensor of the higher order geometrical terms to be treated as anisotropic imperfect fluid with time dependent density function  $\rho(t)$  and radial and tangential pressures  $p_r(t)$  and  $p_t(t)$  respectively. We solved linearized metric equation via perturbation method and obtained 12 different kinds of metric solutions. Calculated Ricci and Kretschmann scalars of our metric solutions are non-singular at beginning of the collapse for 2 kinds of them only. Event and apparent horizons are formed at finite times for two kinds of singular metric solutions while 3 metric solutions exhibit with event horizon only with no formed apparent horizon. There are obtained 3 other kinds of the metric solutions which exhibit with apparent horizon with no formed event horizon. Furthermore 3 kinds of our metric solutions do not exhibit with horizons. Barotropic index of all 12 kinds of metric solutions are calculated also. They satisfy different regimes such as domain walls (6 kinds), cosmic string (2 kinds), dark matter (2 kinds), anti-matter (namely negative energy density) (1 kind) and stiff matter (1 kind). Time dependent radial null geodesics expansion parameter  $\Theta(t)$  is also calculated for all 12 kinds of our metric solutions. In summary 4 kinds of our solutions take absolutely positive value  $\Theta > 0$  which means the collapse ended to a naked singularity but 8 kinds of our metric solutions ended to a covered singularity at end of the collapse where  $\Theta \leq 0$  and so trapped surfaces are appeared.

**Keywords-** Higher order derivative gravity, Anisotropic fluid, Spherically symmetric collapse, Non-singular models, Naked singularity, Domain walls, Cosmic string, Dark matter, Anti-matter, Stiff matter, Trapped surface

## I. INTRODUCTION

Renormalization theory of expectation value of stress energy tensor operator of propagating quantum fields in

curved space-times, leads to some geometrical state independent and also state dependent corrections on right hand side (RHS) of Einstein's gravity equation. State independent geometrical objects are obtained in terms of Lovelock polynomials [1,2] They are made from higher order derivatives of the background metric ' $g_{\mu\nu}$ ' as ' $R^2$ ', ' $\square R$ ', ' $R_{\mu\nu}R^{\mu\nu}$ ' and ' $R_{\mu\nu\gamma\delta}R^{\mu\nu\gamma\delta}$ ', where ' $R$ ', ' $R_{\mu\nu}$ ' and ' $R_{\mu\nu\gamma\delta}$ ' denote as usual the scalar curvature, Ricci and Riemann tensors respectively (see also [3,4]). The basic motivation for studying these *Higher Derivative gravity theories* comes from the fact that they provide one possible approach to an as yet unknown quantum theory of gravity [5]. However, the structure of classical solutions of higher derivative gravity may provide a better approximation to some metric solutions with respect to those provided by general relativity. In four dimensions, due to the Gauss-Bonnet topological invariant, the corresponding Lagrangian contains only two quadratic terms among the above three possible. Cosmological applications of this formalism have been considered mainly in the context of inflationary cosmology, since the R-squared term has the virtue of inducing an early inflationary stage in the spatially homogeneous and isotropic Friedmann-Lemaître-Robertson Walker (FLRW) models (see for instance [6,7]). At the quantum level one can see [8], where the effects of curvature-squared terms is studied on the wave function of the closed FLRW space time by the Hawking and Luttrell. They obtained that Weyl-squared term in the action plays no role while the  $R^2$  term behaves like a massive scalar field. The wave function of the universe can be interpreted as corresponding in the classical limit to a family of solutions that start out with a long period of exponential expansion and then go over to a matter dominated era. Also Wheeler-DeWitt wave equation of quantum cosmology with  $R^2$  term is solved by Kasper [9] (see also [10]). The quantum cosmology of introducing a cubic term in the scalar curvature into the Einstein-Hilbert action was studied previously in the ref. [11]. In the present work we want to study physical effects of the Lovelock polynomials on evolution of ASSC stellar cloud as follows.

We use now the Einstein-Hilbert action added by combinations of the geometrical objects ' $R_{\mu\nu}R^{\mu\nu}$ ', ' $R_{\mu\nu\gamma\delta}R^{\mu\nu\gamma\delta}$ ', and  $R^2$  to characterize structure of interior metric of ASSC star. Here we assume that geometrical source of the modified Einstein's equation treats as classical stress tensor of anisotropic fluid stellar matter with barotropic index  $\gamma = \frac{p}{\rho}$  and anisotropic index  $\Delta = \frac{p_r - p_t}{\rho}$  where  $p_r$  and  $p_t$  are radial and transverse pressures.  $\rho$  and  $p$  are energy density and isotropic pressure.

\*Email address:  
hghafarnejad@yahoo.com  
hghafarnejad@profs.semnan.ac.ir

We solved linearized dynamical metric equation and obtained family of time dependent metric solutions (12 different kinds) and corresponding energy density and all pressures of the collapsed object. Mathematical derivations show that the stellar collapse reaches to covered singularity space time in 7 kinds of our solutions while 5 kinds of them reach to a naked singularity which in the latter cases cosmic censorship conjecture is violated. 10 kinds of our solutions are asymptotically flat but 2 kinds take flat Minkowski form at beginning of the collapse. In the latter 2 cases Ricci and Kretschmann scalars are calculated as regular while in the former 10 cases they become singular at beginning of the collapse. For 2 kinds of our metric solutions the event and apparent horizons are formed at finite times. 4 (3) kinds of our metric solutions exhibit with event (apparent) horizon only at finite times. 3 kinds of our metric solutions do not exhibit with both event and apparent horizons. Details of the work are given as follows.

In section II, we call modified Einstein-Hilbert action functional with additional Lovelock polynomials. In section III, we describe summary of physical properties of an spherically symmetric collapsing star and obtained time dependent, linearized gravitational field equations of anisotropic spherically symmetric time-dependent curved space-time. We assume higher order derivative geometrical counterparts treat as anisotropic imperfect fluid. We obtained 12 different kinds of metric solutions and calculate time dependent energy density, radial, transverse, isotropic and anisotropic pressures, barotropic and anisotropy indexes of collapsing cloud. In section IV we study dynamics of event and apparent horizon formation and also obtained equation of trapped surfaces. In section V we study conditions on radial null geodesics expansion parameter and obtained exactly time dependence of them for all 12 kinds of our metric solutions. Also their diagrams are plotted against collapsing time in figures 1, 2, 3,  $\dots$  12. Also our numerical results are collected at tables 1, 2, 3, 4 and 5. Section VI denotes to concluding remarks.

## II. EFFECTIVE GRAVITY THEORY

Let us we start with the following action functional in which we used units ' $G = c = \hbar = 1$ ' [3,4,5].

$$I = \frac{1}{16\pi} \int dx^4 \sqrt{g} \{ R + \zeta R^2 + \eta R^{\mu\nu} R_{\mu\nu} + \xi R^{\mu\nu\alpha\beta} R_{\mu\nu\alpha\beta} \} \quad (1)$$

where the coupling constants ' $\zeta$ ', ' $\eta$ ' and ' $\xi$ ' come from dimensional regularization of interacting quantum matter fields. They have dimensions as  $(length)^2$  and must be determined by experiment. Hence we solve dynamical field equations against arbitrary values of these parameters and obtain some physical statements. In particular case  $\xi = 1 = \zeta$  and  $\eta = -4$  the above action up to term of Ricci scalar  $R$  become a topological invariant (called the Euler number) and in case  $\zeta = \frac{1}{2}$ ,  $\eta = -2$ ,  $\xi = 1$  it leads

to the well known Weyl-squared scalar  $C^{\mu\nu\eta\delta} C_{\mu\nu\eta\delta}$ . ' $g$ ' is absolute value of determinant of the metric field ' $g_{\mu\nu}$ '. Varying (1), with respect to ' $g^{\mu\nu}$ ', we obtain the metric field equation as (see [3,4,5] and references therein):

$$G_{\mu\nu} = 8\pi T_{\mu\nu} = -(\alpha H_{\mu\nu}^{(1)} + \beta H_{\mu\nu}^{(2)}) \quad (2)$$

where we defined

$$\alpha = \zeta - \xi, \quad \beta = \eta + 4\xi, \quad (3)$$

$$H_{\mu\nu}^{(1)} = 2(\nabla_\mu \nabla_\nu R + R R_{\mu\nu}) - g_{\mu\nu}(2\Box R + \frac{1}{2}R^2) \quad (4)$$

and

$$H_{\mu\nu}^{(2)} = \nabla_\mu \nabla_\nu R - \Box R_{\mu\nu} + 2R^{\alpha\beta} R_{\alpha\beta\mu\nu} - \frac{1}{2}g_{\mu\nu}(\Box R + R^{\alpha\beta} R_{\alpha\beta}). \quad (5)$$

From trace of the metric equation (2), one can obtain a good condition as  $(6\alpha + 2\beta)\Box R + R + 4\beta R^{\alpha\beta} R_{\alpha\beta} = 0$  which help us to rewrite the metric field equation (2) as other form. Stress tensor given in RHS of the metric equation (2) is geometrical counterpart state independent of quantum matter field gravitational source. It will be considered to be treat as anisotropic imperfect fluid. We solve (2) in the next section to obtain interior metric of ASSC star and effective energy density, all pressure components, barotropic and anisotropy indexes of geometrical fluid.

## III. SPHERICALLY SYMMETRIC COLLAPSING STAR

A massive star may be drop below the *Chandrasekhar* or the *Oppenheimer-Volkoff* limits and so it will be collapsed [12,4]. A proper treatment of gravitational collapse would be prohibitively complicated because of its spherical symmetry breaking in the presence of nonzero space-components of four-velocity of the perfect fluid stellar matter. Even for spherically symmetric configurations in which equation of state of the ASSC star ' $p(\rho)$ ' is still stable as ' $\frac{dp}{d\rho} \geq 0$ ', the possible end of the collapse depends on the in-falling sound velocity of the perfect fluid stellar matter  $v_s$ . For a perfect gas the equation of state is  $p = \rho_m RT = \rho_m v_s^2$  in which  $\rho_m$  is energy density,  $R$  is the particular gas constant, and  $v_s$  is the sound velocity of the gas. It is really a characteristic thermal speed of the fluid molecules as  $v_s = \sqrt{RT}$ . In case of cold gas (dust), the fluid molecules move as non-relativistic and one can obtain barotropic index of state equation as  $\gamma = \frac{p}{\rho} = \frac{\rho_m v_s^2}{\rho_m c^2} = \frac{v_s^2}{c^2} \approx 0$ , where  $\rho = \rho_m c^2$  and  $v_s \ll c$ , for a "cold" gas, and  $c$  is speed of light. In case of non-degenerate, ultra-relativistic gas (radiation but also matter in the very early universe) the barotropic

index become  $\gamma = \frac{1}{3}$  because of  $v_s \approx \frac{c}{\sqrt{3}}$  in each direction of 3-space. Usually barotropic index  $\gamma = \frac{p}{\rho}$  is called as  $\gamma$ -law condition on the state equation  $p = \gamma\rho$  which at Zel'dovich interval  $0 < p < \rho$  [13] must be satisfied as

$$0 < \gamma(t) < 1. \quad (6)$$

In the latter situation the mean free path between particle collisions is much less than the scales of physical interest, then the fluid may be treat as perfect. This is also a good approximation to the behavior of any form of non-relativistic fluid or gas. In other words, dust dominance of the stellar perfect fluid is only a hydrostatic fluid which is rest with respect to a comoving coordinate system. In case stiff matter of imperfect fluids the corresponding barotropic index is  $\gamma = 1$  and for supper stiff matter  $\gamma > 1$ . In case  $\gamma = -1$  the fluid is treated as dark energy (the cosmological constant) which can be support acceleration of cosmic inflation. More generally, the expansion of the universe is accelerating for any equation of state  $\gamma < -\frac{1}{3}$  which corresponds to dark energy. If  $\gamma < -1$  the dark energy lies in the phantom regime and would cause a big rip. If  $-1 < \gamma < -\frac{1}{3}$  the dark energy lies in the quintessence regime. Using the existing data, it is still impossible to distinguish between phantom and quintessence. Critical barotropic index  $\gamma = -\frac{1}{3}$  characterizes cosmic string and causes to expands the universe without acceleration. The latter situation can be seen from well known Friedmann equation  $\frac{\ddot{a}}{a} = -\frac{4\pi G}{3}(1+3\gamma)\rho$ . In case  $-\frac{1}{3} < \gamma < 0$  the fluid lies in the dark matter regime. Particular value  $\gamma = -\frac{2}{3}$  characterizes domain wall.

In order to get some feeling for what can happen during collapse, it is considered usually the simplest case named as *Tollman* model [14,15]. In that case, the stellar collapse is assumed to be spherically symmetric inhomogeneous perfect fluid matter. In spherically symmetric space time, without loss of generality, the line element can be written in diagonal form as

$$ds^2 = -e^{2\nu(t,r)} dt^2 + e^{2\lambda(t,r)} dr^2 + R^2(t,r)(d\theta^2 + \sin^2\theta d\varphi^2). \quad (7)$$

The proper radius from center of the collapsing fluid is  $R(t,r)$  and the collapsing boundary surface  $\Sigma$  is given in the interior comoving coordinates as a free fall surface  $r = r_0 = \text{const}$  so that  $R_\Sigma = R(t, r_0)$ . Usually the exterior metric of the collapsing star is assumed to be static and satisfies the standard Darmois-Israel junction conditions (see [16,17] and reference therein).

We know that the geometry inside the collapsing star is dynamic since the radial coordinate become time-like and the metric is time dependent (see also [18]). Hence we choose a non-comoving observer where the interior metric of the ASSC star become

$$ds^2 = -e^{a(t)} dt^2 + e^{b(t)} dr^2 + t^2 e^{c(t)} (d\theta^2 + \sin^2\theta d\varphi^2) \quad (8)$$

where  $a(t), b(t), c(t)$  are determined by solving the metric equation (2). It should be pointed that 2-sphere spatial

part of the above metric is inhomogeneous because of absence of  $r^2$  term. Inserting (8) the components of the tensor equation (2) become nonlinear and so one must be decide to solve (2) by applying one of numerical or perturbative analytical methods. We will consider here the latter method by assuming the following perturbation series expansions to linearize the metric field equation (2).

$$e^{a(t)} = e^{a_0} \{1 + \epsilon a_1(t) + O(\epsilon^2)\}, \quad (9)$$

$$e^{b(t)} = e^{b_0} \{1 + \epsilon b_1(t) + O(\epsilon^2)\} \quad (10)$$

and

$$e^{c(t)} = e^{c_0} \{1 + \epsilon c_1(t) + O(\epsilon^2)\} \quad (11)$$

where  $a_0, b_0, c_0$  are constants and  $\epsilon$  is a suitable dimensionless order parameter of the series expansion. For instance we can choose  $\epsilon = \frac{\alpha}{\beta}$  for  $\alpha < \beta$  or  $\epsilon = \frac{\beta}{\alpha}$  for  $\alpha > \beta$  respectively. In case  $\alpha = \beta$  the equation (3) leads to  $\zeta - \eta = 5\xi$  for which we can choose  $\epsilon = \{\frac{\zeta}{\eta}, \frac{\zeta}{\xi}, \frac{\eta}{\xi}\}$ , for  $\{\zeta < \eta, \zeta < \xi, \eta < \xi\}$  respectively or vice versa. Applying (9), (10) and (11) zero order approximation of the metric equation (2.2) leads to the following condition.

$$e^{a_0} = -e^{c_0} \quad (12)$$

where the line element (8) will be take the following form.

$$ds^2 \simeq -e^{a_0} (1 + \epsilon a_1(t)) dt^2 + e^{b_0} (1 + \epsilon b_1(t)) dr^2 - t^2 e^{a_0} (1 + \epsilon c_1(t)) (d\theta^2 + \sin^2\theta d\varphi^2). \quad (13)$$

First we set

$$a_0 = i\pi, \quad b_0 = 0 \quad (14)$$

because interior metric of the collapsing star has Euclidean signature (+, +, +, +). Applying (9), (10), (11), (12) and (14), first order part of nonzero  $tt, rr, \theta\theta$ , components of the metric equation (2) become respectively

$$\begin{aligned} & (8\alpha + 3\beta)\ddot{c}_1 + (24\alpha + 11\beta)\dot{c}_1/t + (1 - 2\beta/t^2)\dot{c}_1 - (1/t \\ & + (16\alpha + 10\beta)/t^3)c_1 - (8\alpha + 3\beta)\ddot{a}_1/t - (16\alpha + 6\beta)\dot{a}_1/t^2 \\ & - (1/t - (16\alpha + 10\beta)/t^3)a_1 \\ & + 4(2\alpha + \beta)\ddot{b}/t + (1 - 4(2\alpha + \beta)/t^2)\dot{b}_1 = 0, \quad (15) \\ & (4\alpha + \beta)\ddot{c}_1 + (20\alpha + 5\beta)\dot{c}_1/t + ((4\alpha + \beta)/t^2 + 1)\dot{c}_1 + \\ & (2(4\alpha + \beta)/t^3 + 3/t)\dot{c}_1 + (1/t^2 + 2(4\alpha + \beta)/t^4)c_1 \end{aligned}$$

$$\begin{aligned}
& -(4\alpha + \beta)\ddot{a}_1/t - (4\alpha + \beta)\dot{a}_1/t^2 + (1/t - (8\alpha + 2\beta)/t^3)\dot{a}_1 \\
& + (1/t^2 - (8\alpha + 2\beta)/t^4)a_1 + (2\alpha + \beta)\ddot{b}_1 + (12\alpha + 4\beta)\ddot{b}_1/t = 0
\end{aligned} \tag{16}$$

and

$$\begin{aligned}
& (4\alpha + 3\beta)\ddot{c}_1 + (40\alpha + 20\beta)\dot{c}_1/t + (2(4\alpha + 13\beta)/t^2 + 1)\dot{c}_1 \\
& + (2(5\beta - 4\alpha)/t^3 + 2/t)\dot{c}_1 - 2(4\alpha + \beta)c_1/t^4 + (4\alpha + \beta)\ddot{b}_1 \\
& + 2(8\alpha + 3\beta)\ddot{b}_1/t + (4\beta/t^2 + 1)\dot{b}_1 + (2\beta/t^3 + 1/t)\dot{b}_1
\end{aligned}$$

$$-(8\alpha + 4\beta)\ddot{a}_1/t - (8\alpha + 12\beta)\dot{a}_1/t^2$$

$$-(1/t - (8\alpha - 6\beta)/t^3)\dot{a}_1 + (8\alpha + 2\beta)a_1/t^4 = 0. \tag{17}$$

$\varphi\varphi$  component of the metric equation (2) leads to the equation (17) and does not give us more information about the metric solutions. Over dot denotes to differentiations with respect to time parameter 't'.

If we want to know about time dependence of energy density and pressures of the collapsing cloud, we must have Einstein tensor components which up to second order terms  $O(\epsilon^2)$ , are obtained as

$$G_t^t(t) \simeq -\epsilon\{(\dot{c}_1 + \dot{b}_1)/t + (c_1 - a_1)/t^2\}, \tag{18}$$

$$G_r^r(t) \simeq -\epsilon\{\ddot{c}_1 + (3\dot{c}_1 - \dot{a}_1)/t + (c_1 - a_1)/t^2\}, \tag{19}$$

and

$$G_\varphi^\varphi = G_\theta^\theta \simeq -\epsilon\{(\ddot{b}_1 + \ddot{c}_1)/2 + (2\dot{c}_1 + \dot{b}_1 - \dot{a}_1)/2t\} \tag{20}$$

where we insert (12) and (15). Anisotropy property of our gravitational system can be seen from inequality between (19) and (20) as  $G_r^r \neq G_\theta^\theta = G_\varphi^\varphi$ . Hence we assume that right side of the equation (2) describes an imperfect fluid stellar matter source with anisotropic stress tensor

$$T_\mu^\nu = \text{diag}[-\rho(t), p_r(t), p_t(t), p_t(t)] \tag{21}$$

where  $p_r(t)$  and  $p_t(t)$  are radial and transverse (tangential) pressures respectively. We decompose the stress tensor (21) to two parts as

$$T_\mu^\nu = \text{diag}[-\rho, p + \Pi_r^r, p + \Pi_\theta^\theta, p + \Pi_\varphi^\varphi] \tag{22}$$

where  $p(t)$  is isotropic pressure as

$$p(t) = \frac{p_r + 2p_t}{3} \tag{23}$$

and  $\Pi_\mu^\nu$  is traceless anisotropic stress tensor as

$$\Pi_\mu^\nu(t) = (p_r - p_t)\text{diag}\left[0, \frac{2}{3}, -\frac{1}{3}, -\frac{1}{3}\right] \tag{24}$$

which are determined from trace of the tensors (21) and (22). Applying (18), (19), (20) and comparing (21) with (2), one can obtain

$$\rho(t) \simeq \frac{\epsilon}{8\pi}\{(\dot{c}_1 + \dot{b}_1)/t + (c_1 - a_1)/t^2\} \tag{25}$$

$$p_r(t) \simeq -\frac{\epsilon}{8\pi}\{\ddot{c}_1 + (3\dot{c}_1 - \dot{a}_1)/t + (c_1 - a_1)/t^2\}, \tag{26}$$

$$p_t(t) \simeq -\frac{\epsilon}{8\pi}\{(\ddot{b}_1 + \ddot{c}_1)/2 + (2\dot{c}_1 + \dot{b}_1 - \dot{a}_1)/2t\} \tag{27}$$

$$p(t) \simeq -\frac{\epsilon}{24\pi}\{2\ddot{c}_1 + \ddot{b}_1 + 5\dot{c}_1/t + \dot{b}_1/t - \dot{a}_1/t\}. \tag{28}$$

We have also dimensionless anisotropy index

$$\begin{aligned}
\Delta(t) = \frac{(p_t - p_r)}{\rho} & \simeq \{\ddot{c}_1/2 - \ddot{b}_1/2 + 2\dot{c}_1/t - \dot{b}_1/2t - \dot{a}_1/2t \\
& + (c_1 - a_1)/t^2\}/\{(\dot{c}_1 + \dot{b}_1)/t + (c_1 - a_1)/t^2\}
\end{aligned} \tag{29}$$

and dimensionless barotropic index

$$\begin{aligned}
\gamma(t) = \frac{p(t)}{\rho(t)} & \simeq -\frac{1}{3}\{2\ddot{c}_1 + \ddot{b}_1 + 5\dot{c}_1/t + \dot{b}_1/t - \dot{a}_1/t\}/\{(\dot{c}_1 + \dot{b}_1)/t \\
& + (c_1 - a_1)/t^2\}.
\end{aligned} \tag{30}$$

If we want to know about singularity of our obtained metric solutions we must determine corresponding Ricci and Kretschmann scalars which up to second order terms become respectively

$$R = R_\lambda^\lambda = \epsilon\{\ddot{b}_1 + 2\ddot{c}_1 + 2(3\dot{c}_1 + \dot{b}_1 - \dot{a}_1)/t + 2(c_1 - a_1)/t^2\} \tag{31}$$

and

$$\begin{aligned}
K = R_{\mu\nu\eta\delta}R^{\mu\nu\eta\delta} & = \epsilon^2\{\ddot{b}_1^2 + (3/2)(\dot{c}_1 + (2\dot{c}_1 - \dot{a}_1)/t)^2 \\
& + 2\dot{b}_1^2/t^2 + 24(\dot{c}_1/t + (c_1 - a_1)/t^2)^2\}.
\end{aligned} \tag{32}$$

Up to second order terms, one can calculate covariant conservation condition of the stress tensor (21) given by  $\nabla_\mu T_\nu^\mu = 0$  as

$$\begin{aligned}
\dot{\rho} + (2/t + \epsilon(\dot{b}_1 + 2\dot{c}_1)/2)(\rho + p) & \simeq (1/3)(p_r - p_t)(2/t \\
& + \epsilon(\dot{c}_1 - \dot{b}_1)).
\end{aligned} \tag{33}$$

Inserting (25), (26), (27) and (28) the above conservation condition leads to the following form.

$$3\dot{c}_1 - \dot{a}_1 - (2c_1 + a_1)/t \simeq 0. \tag{34}$$

Coefficients of linearized differential equations (15), (16) and (17) have singularity at time  $t = 0$  and so it will be useful to obtain time dependent metric solutions  $(a_1, b_1, c_1)$  at neighborhood  $t \rightarrow 0$ . Also we need to fix initial conditions on the obtained solution. We will consider two different initial conditions as  $a_1(0) = b_1(0) = c_1(0) = 0$  and  $a_1(\infty) = b_1(\infty) = c_1(\infty) = 0$  and obtain two class of metric solutions which are flat Minkowski at  $t = 0$  and  $t \rightarrow \infty$  respectively.

Asymptotically behavior of the equations (15), (16) and (17) at  $t \rightarrow 0$  are respectively

$$\begin{aligned} (8 + 3\omega)\ddot{c}_1 + \frac{(24 + 11\omega)}{t}\dot{c}_1 - \frac{2\omega}{t^2}\dot{c}_1 - \frac{(16 + 10\omega)}{t^3}c_1 \\ + \frac{4(2 + \omega)}{t}\dot{b}_1 - \frac{4(2 + \omega)}{t^2}b_1 \\ - \frac{(8 + 3\omega)}{t}\ddot{a}_1 - \frac{(16 + 6\omega)}{t^2}\dot{a}_1 + \frac{(16 + 10\omega)}{t^3}a_1 \approx 0, \quad (35) \\ (4 + \omega)\ddot{c}_1 + \frac{(20 + 5\omega)}{t}\dot{c}_1 + \frac{(4 + \omega)}{t^2}\dot{c}_1 + \frac{2(4 + \omega)}{t^3}c_1 \\ + \frac{2(4 + \omega)}{t^4}c_1 + (2 + \omega)\ddot{b}_1 + \frac{(12 + 4\omega)}{t}\dot{b}_1 - \frac{(4 + \omega)}{t}\ddot{a}_1 \\ - \frac{(4 + \omega)}{t^2}\dot{a}_1 - \frac{(8 + 2\omega)}{t^3}\dot{a}_1 - \frac{(8 + 2\omega)}{t^4}a_1 \approx 0 \quad (36) \end{aligned}$$

and

$$\begin{aligned} (4 + 3\omega)\ddot{c}_1 + \frac{(40 + 20\omega)}{t}\dot{c}_1 + \frac{2(4 + 13\omega)}{t^2}\dot{c}_1 + \frac{2(5\omega - 4)}{t^3}c_1 \\ - \frac{2(4 + \omega)}{t^4}c_1 + (4 + \omega)\ddot{b}_1 + \frac{2(8 + 3\omega)}{t}\dot{b}_1 + \frac{4\omega}{t^2}\dot{b}_1 + \frac{2\omega}{t^3}b_1 \\ - \frac{(8 + 4\omega)}{t}\ddot{a}_1 - \frac{(8 + 12\omega)}{t^2}\dot{a}_1 + \frac{(8 - 6\omega)}{t^3}\dot{a}_1 \\ + \frac{(8 + 2\omega)}{t^4}a_1 \approx 0 \quad (37) \end{aligned}$$

where we defined dimensionless parameter  $\omega$  as

$$\omega = \frac{\beta}{\alpha} = \frac{\eta + 4\xi}{\zeta - \xi}. \quad (38)$$

The equations (35), (36) and (37) have power-law solutions as

$$a_1(t) \simeq A \left( \frac{t}{\sqrt{\alpha}} \right)^\mu, \quad b_1(t) \simeq B \left( \frac{t}{\sqrt{\alpha}} \right)^\mu, \quad c_1(t) \simeq E \left( \frac{t}{\sqrt{\alpha}} \right)^\mu \quad (39)$$

in which the constants  $A, B, E$  and  $\mu$  are related to  $\omega$ . They are obtained by inserting (39) into the equations (35), (36) and (37) as follows.

$$\begin{aligned} \frac{A}{B} = \{ \omega^2(-3\mu^7 + 8\mu^6 + 2\mu^5 - 12\mu^4 + 13\mu^3 + 28\mu^2 - 108\mu) \\ - \omega(14\mu^7 - 36\mu^6 + 28\mu^4 - 102\mu^3 + 168\mu^2 + 104\mu) \\ - 16\mu^7 + 32\mu^6 + 32\mu^5 - 96\mu^4 + 240\mu^3 - 448\mu^2 + 192\mu \} / \{ \omega^2 \\ \times (4\mu^5 - 20\mu^4 + 90\mu^2 + 42\mu - 140) \\ + \omega(32\mu^5 - 144\mu^4 + 16\mu^3 + 276\mu^2 + 88\mu - 144) \\ + (64\mu^5 - 256\mu^4 + 64\mu^3 + 320\mu^2 - 64\mu + 128) \} \quad (40) \end{aligned}$$

$$\begin{aligned} \frac{E}{B} = -\{ \omega^2(7\mu^6 + 365\mu^5 - 1923\mu^4 + 3107\mu^3 - 1536\mu^2 - 36\mu) \\ + \omega(36\mu^6 + 606\mu^5 - 3526\mu^4 + 5738\mu^3 - 2704\mu^2 - 248\mu) + 48\mu^6 \\ - 240\mu^5 + 624\mu^4 - 944\mu^3 + 704\mu^2 - 320\mu \} / \{ \omega^2(4\mu^5 - 20\mu^4 \\ + 90\mu^2 + 42\mu - 140) + \omega(32\mu^5 - 144\mu^4 + 16\mu^3 + 276\mu^2 + 88\mu \\ - 144) + 64\mu^5 - 256\mu^4 + 64\mu^3 + 320\mu^2 - 64\mu + 128 \} \quad (41) \end{aligned}$$

and

$$\begin{aligned} \omega^3 \{ 320\mu^9 - 960\mu^8 - 3520\mu^7 + 29440\mu^6 - 80896\mu^5 + 111936\mu^4 \\ - 92352\mu^3 + 52800\mu^2 - 10880\mu - 2048 \} + \omega^2 \{ 33\mu^9 + 1073\mu^8 \\ - 5104\mu^7 + 5658\mu^6 + 4611\mu^5 - 19253\mu^4 + 28128\mu^3 - 14094\mu^2 \\ - 5308\mu + 3648 \} + \omega \{ 464\mu^9 + 1544\mu^8 - 4984\mu^7 - 63368\mu^6 \\ + 304688\mu^5 - 540776\mu^4 + 441036\mu^3 - 149624\mu^2 + 12944\mu \\ + 3456 \} + 216\mu^9 + 3158\mu^8 - 11818\mu^7 - 27952\mu^6 + 182054\mu^5 \\ - 336406\mu^4 + 298530\mu^3 - 115962\mu^2 + 236\mu + 8672 = 0 \quad (42) \end{aligned}$$

Inserting (39) the conservation equation (34) leads to the following condition.

$$(3\mu - 2)E - (1 + \mu)A = 0. \quad (43)$$

Inserting (40) and (41), the latter equation can be rewritten as

$$\begin{aligned} & \omega^2(3\mu^7 - 26\mu^6 - 1091\mu^5 + 6509\mu^4 - 13168\mu^3 + 10781\mu^2 \\ & - 2884\mu + 36) + \omega(14\mu^7 - 130\mu^6 - 1782\mu^5 + 11818\mu^4 - 24340\mu^3 \\ & + 19654\mu^2 - 4392\mu - 392) + 16\mu^7 - 160\mu^6 \\ & + 752\mu^5 - 2288\mu^4 + 3936\mu^3 - 3792\mu^2 + 2624\mu - 832 = 0. \end{aligned} \quad (44)$$

One can solve (42) and (44) simultaneously to obtain numerical values of the parameters  $\mu$  and  $\omega$ . We plotted diagrams of the equations (42) and (44) at figure 1 where crossing points determine numerical values of the parameters  $\mu$  and  $\omega$ . There are 12 crossing points called as  $P_i \equiv (\mu_i, \omega_i)$ ;  $i = 1, 2, 3 \dots 12$  and collected at first and second column at table 1.

Inserting (12), (14) and (39) one can obtain explicit form of the line element (13), the barotropic index (29) and the anisotropy index (30) respectively as

$$\begin{aligned} ds^2 \approx & \left[ 1 + \frac{A}{B} \left( \frac{t}{\sqrt{\alpha}} \right)^\mu \right] dt^2 + \left[ 1 + \left( \frac{t}{\sqrt{\alpha}} \right)^\mu \right] dr^2 \\ & + t^2 \left[ 1 + \frac{E}{B} \left( \frac{t}{\sqrt{\alpha}} \right)^\mu \right] (d\theta^2 + \sin^2 \theta d\varphi^2) \end{aligned} \quad (45)$$

$$\Delta(t) \approx \frac{(2\mu^2 + 3\mu + 1)\frac{E}{B} - (1 + 2\mu)\frac{A}{B} - \mu}{2(1 + \mu)\frac{E}{B} - 2\frac{A}{B} + 2\mu} \quad (46)$$

and

$$\gamma(t) \approx -\frac{1}{3} \left[ \frac{\frac{A}{B} - (3 + 2\mu)\frac{E}{B} - \mu}{\frac{A}{B} - (1 + \mu)\frac{E}{B} - \mu} \right] \quad (47)$$

where we set

$$\epsilon = \frac{1}{B}. \quad (48)$$

Inserting numerical values of the parameters  $\mu_i, \omega_i$  given in the table 1 one can obtain numerical values of the coefficients  $\frac{A}{B}, \frac{E}{B}, \Delta(t)$  and  $\gamma(t)$  for all 12 points  $P_i$ . They are collected also at the figure 1.

Inserting (39) we can rewrite the equations (25), (26), (27), (28), (32) and (33) as follows.

$$\begin{aligned} \frac{\rho(t)}{\rho(\sqrt{\alpha})} & \approx \left( \frac{t}{\sqrt{\alpha}} \right)^{\mu-2} = \frac{p_r(t)}{p_r(\sqrt{\alpha})} = \frac{p_t(t)}{p_t(\sqrt{\alpha})} = \frac{p(t)}{p(\sqrt{\alpha})} \\ & = \frac{R_\lambda^\lambda(t)}{R_\lambda^\lambda(\sqrt{\alpha})} = \sqrt{\frac{K(t)}{K(\sqrt{\alpha})}} \end{aligned} \quad (49)$$

where we defined

$$\rho^* = 8\pi\alpha\rho(\sqrt{\alpha}) = \left[ 1 - \frac{A}{B} + (1 + \mu)\frac{E}{B} \right] \quad (50)$$

$$p_r^* = 8\pi\alpha p_r(\sqrt{\alpha}) = (1 + \mu) \left[ \frac{A}{B} - (1 + \mu)\frac{E}{B} \right] \quad (51)$$

$$p_t^* = 8\pi\alpha p_t(\sqrt{\alpha}) = \frac{\mu}{2} \left[ \frac{A}{B} - (1 + \mu)\frac{E}{B} - \mu \right] \quad (52)$$

$$p^* = 8\pi\alpha p(\sqrt{\alpha}) = \frac{\mu}{3} \left[ \frac{A}{B} - (3 + 2\mu)\frac{E}{B} - \mu \right] \quad (53)$$

$$R^* = \alpha R_\lambda^\lambda(\sqrt{\alpha}) = (1 + \mu) \left[ \mu - 2\frac{A}{B} + 2(1 + \mu)\frac{E}{B} \right] \quad (54)$$

$$\begin{aligned} K^* = \alpha^2 K(\sqrt{\alpha}) & = \left[ \mu^2(\mu^2 - 2\mu + 3) + 25 \left( \frac{A}{B} \right)^2 \right. \\ & \left. + (1 + \mu)^2 [24 + 3\mu^2/2] \left( \frac{E}{B} \right)^2 - 2(24 + \mu)(1 + \mu) \left( \frac{E}{B} \right) \left( \frac{A}{B} \right) \right]. \end{aligned} \quad (55)$$

Numerical values of the parameters (50), (51), (52), (53), (54) and (55) are calculated at the particular points  $P_i$ ;  $i = 1, 2, 3, \dots 12$  and are collected in table 2. In the next section we proceed to obtain the times where internal event and apparent horizons of our obtained metric solutions are formed.

#### IV. HORIZONS FORMATION AND TRAPPED SURFACES

Here we assume the existence of an apparent horizon, which is defined as the outer boundary of a connected component of the trapped region. The important feature of the apparent horizon is that, if the space time is strongly asymptotically predictable and the null convergence condition holds, the presence of the apparent horizon implies the desistance of an event horizon outside or coinciding with it. If the connected component of the trapped region has the structure of a manifold with boundaries, then the apparent horizon is an outer marginally trapped surface with vanishing expansion [19]. Along a future directed outgoing null geodesic, the relation [20]

$$\begin{aligned} \frac{dR}{dt} & = \partial_t R + \partial_r R \frac{dr}{dt} \\ & = e^\nu \left( e^{-\lambda} \partial_r R \pm \sqrt{-1 + \frac{2m}{R} + e^{-2\lambda} (\partial_r R)^2} \right) \end{aligned} \quad (56)$$

for line element (7) is satisfied, where  $+(-)$  corresponds to expanding (collapsing) phase and

$$m(t, r) = \frac{R}{2} (1 - e^{-2\lambda} (\partial_r R)^2 + e^{-2\nu} (\partial_t R)^2) \quad (57)$$

is the Misner-Sharp mass function [21]. Assuming  $\partial_r R > 0$  the equation (56) shows that in the expanding phase there is no apparent horizon but in the collapsing phase on a hypersurface of constant  $t$  the two-sphere  $R = 2m$  is an apparent horizon. The region  $R < 2m$  is trapped surfaces where  $\frac{dR}{dt} < 0$ , while the region  $R > 2m$  is not trapped in which  $\frac{dR}{dt} > 0$ . Singularities which can be appeared in spherically collapse are called ‘shell-crossing’ if  $\partial_r R = 0$  with  $R > 0$  and ‘shell-focusing’ if  $R = 0$ . In the local frame, the space time may to be has ‘central-singularity’ and ‘non-central singularity’ which is characterized by  $r = 0$  and  $r > 0$  respectively. In the metric solution (45) time dependent 2-sphere radiuses are

$$R(t, r) = t \sqrt{1 + \frac{E}{B} \left( \frac{t}{\sqrt{\alpha}} \right)^\mu} \quad (58)$$

in which  $\partial_r R = 0$  and so all hypersurfaces  $R > 0$  are shell-crossing type of space time singularity. Also the particular hypersurfaces

$$t_1 = 0, \quad t_2 = \sqrt{\alpha} \left( -\frac{B}{E} \right)^{\frac{1}{\mu}} \quad (59)$$

which are solutions of the equation  $R(t) = 0$  are shell-focusing singularity of our metric solution. Trapped surfaces are determined by equating  $\frac{dR}{dt} \leq 0$  as

$$R(t) = \text{constant}, \quad 0 \leq \left( \frac{t}{\sqrt{\alpha}} \right) \leq \frac{T_{AH}}{\sqrt{\alpha}} \quad (60)$$

in which

$$\frac{T_{AH}}{\sqrt{\alpha}} = \left[ \left( \frac{-2}{2+\mu} \right) \frac{B}{E} \right]^{\frac{1}{\mu}} \quad (61)$$

is apparent horizon formation time obtained from  $\frac{dR}{dt} = 0$  with corresponding radius

$$\frac{R(T_{AH})}{\sqrt{\alpha}} = \left[ \left( \frac{-2}{2+\mu} \right) \frac{B}{E} \right]^{\frac{1}{\mu}} \sqrt{\frac{\mu}{2+\mu}}. \quad (62)$$

Event horizon formation time  $T_{EH}$  is determined by solving the equation  $g_{tt}(t) = 0$  given by (45) as

$$\frac{T_{EH}}{\sqrt{\alpha}} = \left( -\frac{A}{B} \right)^{-\frac{1}{\mu}} \quad (63)$$

with corresponding 2-sphere radiuses

$$\frac{R(T_{EH})}{\sqrt{\alpha}} = \left( -\frac{B}{A} \right)^{\frac{1}{\mu}} \sqrt{1 - \frac{E}{A}}. \quad (64)$$

Black holes are formed with total Misner-Sharp mass  $M = m(T_{AH})$  and radius  $R(T_{AH})$  if

$$R_{EH} \geq R_{AH} \quad (65)$$

which by inserting (62) and (64) leads to

$$\sigma = \frac{E}{A} + \left( \frac{2}{2+\mu} \right)^{2\mu} \left( \frac{\mu}{2+\mu} \right) - 1 \geq 0. \quad (66)$$

If our metric solutions given by  $P_i$ ;  $i = 1, 2, 3, \dots, 12$  at table 1 can not satisfy the above condition then they will be describe formation of naked singularity at end of collapse. Numerical values of the quantity  $\sigma$  are given in the table 3 for all our metric solutions. The choice  $P_3$  describes a collapsing cloud which reaches finally to a covered singularity by standing apparent horizon and forming event horizon after than that with larger radius. Other cases  $P_i$ ;  $i \neq 3$  given in the table 3 may show naked singularity as end of the collapse. But since the absence of an apparent horizon does not necessary implies the absence of an event horizon, thus we seek naked singularity formation or otherwise also by evaluating time dependence of radial null geodesic expansion parameter as follows. It will be help us to determine nakedness of singularity of other metric solutions denoted with  $P_i$ ;  $i \neq 3$  via studding of trapped surfaces in the following section. Our results are collected in the table 4.

## V. CONDITIONS ON RADIAL NULL GEODESIC EXPANSION

Consider a congruence of outgoing radial null geodesics having the tangent vector  $(V^t(\tau), V^r(\tau), 0, 0)$ , where

$$V^t(\tau) = \frac{dt}{d\tau}, \quad V^r(\tau) = \frac{dr}{d\tau} \quad (67)$$

and  $\tau$  is an affine parameter, along the geodesics. In terms of these two vector fields the geodesic equation can be written as

$$\frac{d \ln V^t}{d\tau} = - \left\{ \left( \frac{\mu}{\sqrt{\alpha}} \right) \left( \frac{A}{B} \right) \frac{\left( \frac{t}{\sqrt{\alpha}} \right)^{\mu-1}}{1 + \frac{A}{B} \left( \frac{t}{\sqrt{\alpha}} \right)^\mu} \right\} V^t \quad (68)$$

and

$$\frac{d \ln V^r}{d\tau} = - \left\{ \left( \frac{\mu}{\sqrt{\alpha}} \right) \frac{\left( \frac{t}{\sqrt{\alpha}} \right)^{\mu-1}}{1 + \left( \frac{t}{\sqrt{\alpha}} \right)^\mu} \right\} V^t. \quad (69)$$

The above equations show that

$$\frac{\partial V^t}{\partial r} = 0, \quad \frac{\partial V^r}{\partial r} = 0. \quad (70)$$

The geodesic expansion parameter is defined by  $\Theta = \nabla_\mu V^\mu = \partial_\mu V^\mu + \Gamma_{\mu\nu}^\mu V^\nu$  which by applying (70) and our metric solution (45) reduces to the following form.

$$\Theta = \frac{\partial V^t}{\partial t} + \frac{\Omega(t) V^t}{2\sqrt{\alpha}} \quad (71)$$

where

$$\begin{aligned} \Omega(t) = & \left(\frac{t}{\sqrt{\alpha}}\right)^{-1} \left\{ 2 + \left[ 3\left(1 + \frac{A}{B}\right) + (2 + \mu)\frac{E}{B} \right] \left(\frac{t}{\sqrt{\alpha}}\right)^\mu \right. \\ & + \left[ 4\frac{A}{B} + (4 + \mu)\frac{E}{A} + (2 + \mu)\frac{AE}{B^2} \right] \left(\frac{t}{\sqrt{\alpha}}\right)^{2\mu} + \frac{EA}{B^2}(2 + \mu) \\ & \left. \times \left(\frac{t}{\sqrt{\alpha}}\right)^{3\mu} \right\} / \left\{ \left[ 1 + \left(\frac{t}{\sqrt{\alpha}}\right)^\mu \right] \left[ 1 + \frac{A}{B} \left(\frac{t}{\sqrt{\alpha}}\right)^\mu \right] \left[ 1 + \frac{E}{B} \left(\frac{t}{\sqrt{\alpha}}\right)^\mu \right] \right\}. \end{aligned} \quad (72)$$

First term of RHS of the equation (71) can be rewritten as

$$\frac{dV^t}{d\tau} = \frac{\partial V^t}{\partial t} \frac{\partial t}{\partial \tau}. \quad (73)$$

Inserting (67) into the above relation one can result

$$\frac{\partial V^t}{\partial t} = \frac{d \ln V^t}{d\tau}. \quad (74)$$

Inserting (68) and (74) we can rewrite the geodesics expansion parameter (71) such as follows.

$$\Theta = \frac{\Xi(t)}{2\sqrt{\alpha}} V^t \quad (75)$$

where we defined

$$\begin{aligned} \Xi(t) = & \left(\frac{t}{\sqrt{\alpha}}\right)^{-1} \left\{ 2 + \left[ 3 + (3 - 2\mu)\frac{A}{B} + (2 + \mu)\frac{E}{B} \right] \left(\frac{t}{\sqrt{\alpha}}\right)^\mu \right. \\ & + \left[ 2(2 - \mu)\frac{A}{B} + (4 + \mu)\frac{E}{A} + (2 - \mu)\frac{AE}{B^2} \right] \left(\frac{t}{\sqrt{\alpha}}\right)^{2\mu} + \frac{EA}{B^2}(2 - \mu) \\ & \left. \times \left(\frac{t}{\sqrt{\alpha}}\right)^{3\mu} \right\} / \left\{ \left[ 1 + \left(\frac{t}{\sqrt{\alpha}}\right)^\mu \right] \left[ 1 + \frac{A}{B} \left(\frac{t}{\sqrt{\alpha}}\right)^\mu \right] \left[ 1 + \frac{E}{B} \left(\frac{t}{\sqrt{\alpha}}\right)^\mu \right] \right\}. \end{aligned} \quad (76)$$

Radial ingoing (-) and outgoing (+) null geodesics of the metric solutions (45) are obtained by setting  $ds = 0 = d\theta = d\varphi$  as

$$\frac{V^t}{V^r} = \frac{dt}{dr} = \pm \sqrt{-\left(\frac{1 + \left(\frac{t}{\sqrt{\alpha}}\right)^\mu}{1 + \frac{A}{B} \left(\frac{t}{\sqrt{\alpha}}\right)^\mu}\right)} \quad (77)$$

where we use (67). Eliminating 't' and  $\tau$  parameters between (68), (69) and (77) we obtain

$$d\left(\frac{1}{(V^t)^2} - \frac{A}{B} \frac{1}{(V^r)^2}\right) = 0 \quad (78)$$

which leads to the following relation.

$$\frac{1}{(V^t)^2} - \frac{A}{B} \frac{1}{(V^r)^2} = \Upsilon = \text{constant}. \quad (79)$$

Using the above relation we can choose

$$V^t(\tau) = \frac{1}{\sqrt{\Upsilon}} \frac{1}{\cosh \tau}, \quad V^r(\tau) = \sqrt{\frac{A}{B\Upsilon}} \frac{1}{\sinh \tau} \quad (80)$$

where

$$\tanh(\tau) = \pm \sqrt{-\left(\frac{\frac{A}{B} + \frac{A}{B} \left(\frac{t}{\sqrt{\alpha}}\right)^\mu}{1 + \frac{A}{B} \left(\frac{t}{\sqrt{\alpha}}\right)^\mu}\right)}. \quad (81)$$

Using (80) and (81) we obtain

$$V^t(t) = \frac{1}{\sqrt{\Upsilon}} \sqrt{\frac{1 + \frac{A}{B} + 2\frac{A}{B} \left(\frac{t}{\sqrt{\alpha}}\right)^\mu}{1 + \frac{A}{B} \left(\frac{t}{\sqrt{\alpha}}\right)^\mu}} \quad (82)$$

and

$$V^r(t) = \frac{\pm 1}{\sqrt{\Upsilon}} \sqrt{\frac{1 + \frac{A}{B} + 2\frac{A}{B} \left(\frac{t}{\sqrt{\alpha}}\right)^\mu}{-(1 + \left(\frac{t}{\sqrt{\alpha}}\right)^\mu)}}. \quad (83)$$

Inserting (82), the geodesics expansion parameter (75) can be rewritten as

$$\begin{aligned} \Theta^*(t) = & 2\sqrt{\alpha}\Sigma\Theta(t) = \left(\frac{t}{\sqrt{\alpha}}\right)^{-1} \sqrt{\frac{1 + \frac{A}{B} + 2\frac{A}{B} \left(\frac{t}{\sqrt{\alpha}}\right)^\mu}{1 + \frac{A}{B} \left(\frac{t}{\sqrt{\alpha}}\right)^\mu}} \\ & \times \left\{ 2 + \left[ 3 + (3 - 2\mu)\frac{A}{B} + (2 + \mu)\frac{E}{B} \right] \left(\frac{t}{\sqrt{\alpha}}\right)^\mu + \left[ 2(2 - \mu)\frac{A}{B} \right. \right. \\ & \left. \left. + (4 + \mu)\frac{E}{B} + (2 - \mu)\frac{AE}{B^2} \right] \left(\frac{t}{\sqrt{\alpha}}\right)^{2\mu} + \frac{EA}{B^2}(2 - \mu)\left(\frac{t}{\sqrt{\alpha}}\right)^{3\mu} \right\} / \\ & \left\{ \left[ 1 + \left(\frac{t}{\sqrt{\alpha}}\right)^\mu \right] \left[ 1 + \frac{A}{B} \left(\frac{t}{\sqrt{\alpha}}\right)^\mu \right] \left[ 1 + \frac{E}{B} \left(\frac{t}{\sqrt{\alpha}}\right)^\mu \right] \right\} \end{aligned} \quad (84)$$

where when  $\Theta > 0$  the singularity become visible and so cosmic censorship conjecture is violated but not for  $\Theta \leq 0$ . In the latter case trapped surfaces appear and their boundary surface region called as apparent horizon is determined by  $\Theta = 0$ . Namely all trapped surfaces satisfy  $\Theta < 0$ . These surfaces are closed orientable smooth two dimensional space-like surfaces such that both families of ingoing and outgoing null geodesics orthogonal to them necessarily converge. The singularity is called naked if there exist a family of future directed non-space-like geodesics reaching faraway observers in space-time and terminating at the singularity in the past with a definite tangent. If such family of curves do not exist and the event horizon forms earlier than the singularity covering it, a black hole is formed. We should point that the absence of an apparent horizon dose not necessarily implies the absence of an event horizon. Some of our obtained metric solutions exhibit with event horizon formation while an apparent horizon can not to form (see



table 3). Inserting numerical values of the parameters  $\{\mu_i, (A/B)_i, (E/B)_i\}$  from the table 1 we obtain exact form of the null geodesics expansion parameter  $\Theta^*(t)_i$  for  $i = 1, 2, 3, \dots, 12$  respectively as follows.

$$\Theta_1^*(t) = \frac{1}{T} \sqrt{\frac{2.45 + 2.9T^{2.433}}{1 + 1.45T^{2.433}}} \times \frac{(2 + 4.812T^{2.433} + 4.660T^{4.866} - 0.640T^{7.299})}{(1 + T^{2.433})(1 + 1.45T^{2.433})(1 + 1.019T^{2.433})} \quad (85)$$

$$\Theta_2^*(t) = \frac{1}{T} \sqrt{\frac{1.029 + 0.058T^{2.057}}{1 + 0.029T^{2.057}}} \times \frac{(2 + 2.907T^{2.057} - 0.094T^{4.114} + 0.00003T^{6.171})}{(1 + T^{2.057})(1 + 0.029T^{2.057})(1 - 0.015T^{2.057})} \quad (86)$$

$$\Theta_3^*(t) = \frac{1}{T} \sqrt{\frac{0.826 - 0.348T^{1.888}}{1 - 0.174T^{1.888}}} \times \frac{(2 + 2.404T^{1.888} - 1.142T^{3.776} + 0.004T^{5.664})}{(1 + T^{1.888})(1 - 0.174T^{1.888})(1 - 0.188T^{1.888})} \quad (87)$$

$$\Theta_4^*(t) = \frac{1}{T} \sqrt{\frac{2.633 + 3.266T^{1.616}}{1 + 1.633T^{1.616}}} \times \frac{(2 + 8.291T^{1.616} + 11.043T^{3.232} + 0.983T^{4.848})}{(1 + T^{1.616})(1 + 1.633T^{1.616})(1 + 1.568T^{1.616})} \quad (88)$$

$$\Theta_5^*(t) = \frac{1}{T} \sqrt{\frac{0.999 - 0.002T^{0.644}}{1 - 0.001T^{0.644}}} \times \frac{(2 + 3.778T^{0.644} + 1.367T^{1.288} - 0.0004T^{1.932})}{(1 + T^{0.644})(1 - 0.001T^{0.644})(1 + 0.295T^{0.644})} \quad (89)$$

$$\Theta_6^*(t) = \frac{1}{T} \sqrt{\frac{2.478 + 2.956T^{0.521}}{1 + 1.478T^{0.521}}} \times \frac{(2 - 6.162T^{0.521} - 27.701T^{1.042} - 10.453T^{1.563})}{(1 + T^{0.521})(1 + 1.478T^{0.521})(1 - 4.782T^{0.521})} \quad (90)$$

$$\Theta_7^*(t) = \frac{1}{T} \sqrt{\frac{0.696 - 0.608T^{0.508}}{1 - 0.304T^{0.508}}} \times \frac{(2 + 5.121T^{0.508} + 3.496T^{1.016} - 0.493T^{1.524})}{(1 + T^{0.508})(1 - 0.304T^{0.508})(1 + 1.086T^{0.508})} \quad (91)$$

$$\Theta_8^*(t) = \frac{1}{T} \sqrt{\frac{0.972 - 0.056T^{-0.041}}{1 - 0.028T^{-0.041}}} \times \frac{(2 + 2.896T^{-0.041} - 0.149T^{-0.082} + 0.0005T^{-0.123})}{(1 + T^{-0.041})(1 - 0.028T^{-0.041})(1 - 0.009T^{-0.041})} \quad (92)$$

$$\Theta_9^*(t) = \frac{1}{T} \sqrt{\frac{1.389 + 0.778T^{-0.201}}{1 + 0.389T^{-0.201}}} \times \frac{(2 + 3.115T^{-0.201} - 1.416T^{-0.402} - 0.575T^{-0.603})}{(1 + T^{-0.201})(1 + 0.389T^{-0.201})(1 - 0.672T^{-0.201})} \quad (93)$$

$$\Theta_{10}^*(t) = \frac{1}{T} \sqrt{\frac{0.956 - 0.088T^{-0.270}}{1 - 0.044T^{-0.270}}} \times \frac{(2 + 2.763T^{-0.270} - 0.370T^{-0.540} + 0.005T^{-0.810})}{(1 + T^{-0.270})(1 - 0.044T^{-0.270})(1 - 0.047T^{-0.270})} \quad (94)$$

$$\Theta_{11}^*(t) = \frac{1}{T} \sqrt{\frac{4.467 + 6.934T^{-3.284}}{1 + 3.467T^{-3.284}}} \times \frac{(2 + 37.892T^{-3.284} + 11.151T^{-6.568} - 24.530T^{-9.852})}{(1 + T^{-3.284})(1 + 3.467T^{-3.284})(1 - 1.339T^{-3.284})} \quad (95)$$

$$\Theta_{12}^*(t) = \frac{1}{T} \sqrt{\frac{8.146 + 18.292T^{-6.206}}{9.146T^{-6.206} - 1}} \times \frac{(2 - 127.892T^{-6.206} + 37.865T^{-12.412} + 182.602T^{-18.616})}{(1 + T^{-6.206})(1 - 9.146T^{-6.206})(1 - 2.433T^{-6.206})} \quad (96)$$

where we defined

$$T = \frac{t}{\sqrt{\alpha}}. \quad (97)$$

Diagrams of the null geodesics expansion parameter  $\Theta_i^*(t)$ ;  $i = 1, 2, 3, \dots, 12$  are plotted at figures 1, 2, 3,  $\dots, 12$  respectively against  $t$ . and their descriptions are given as follows.

**Figure 2.** Diagram crosses horizontal axis at  $T_1 = 2.383$  and  $T \rightarrow \infty$  (thee singularity). Trapped surfaces is characterized for times  $2.383 < T < \infty$  and so the singularity is located inside of trapped surfaces. Thus final state of the collapse is covered singularity as big black hole.

**Figure 3.** Diagram crosses the horizontal axis at  $T_1 = 5.818$ ,  $T_2 = 7.665$  and  $T_3 \rightarrow \infty$  (the singularity).  $\Theta_2^*$  takes negative values for  $5.818 < T < 7.665$  where trapped surfaces are happened and positive values for  $7.665 < T < \infty$ . So the singularity is located outside of trapped surfaces. Thus final state of collapse is naked singularity.

**Figure 4.** Here  $\Theta_3^*$  takes positive values for finite times  $0 < T < 1.707$  (apparent horizon formation time) and it takes negative values (trapped surfaces) for times  $T > 2.536$  (event horizon formation time) and so the trapped surfaces located inside of trapped surfaces. Thus final state of the collapse reaches to a covered singularity (black hole).

**Figure 5.** Here  $\Theta_4^* > 0$  and so there is not trapped surfaces and so final state of the collapse reaches to a naked singularity.

**Figure 6.** Here  $\Theta_5^* > 0$  and so there is not trapped surfaces and so final state of the collapse reaches to a naked singularity.

**Figure 7.** Here  $\Theta_6^* > 0$  for  $0 < T < 0.036$  and  $T \geq 0.05$  while it takes negative values for  $0.036 < T < 0.05$ . Singularity is  $T = 0$  and so it become invisible from distant observers.

**Figure 8.** Here  $\Theta_7^* > 0$  for finite times  $0 < T < 1.334$  and so there is not trapped surfaces and thus the singularity  $T = 0$  become visible from view of distant observers.

**Figure 9.** Here  $\Theta_8^* > 0$  and so there is not trapped surfaces and so final state of the collapse reaches to a naked singularity.

**Figure 10.** Here  $\Theta_9^* > 0$  for  $0 < T < 0.058$  and  $T \geq 0.139$  while it takes negative values for  $0.058 < T < 0.139$ . Singularity is  $T = 0$  and so it become invisible from distant observers.

**Figure 11.** Here  $\Theta_{10}^* > 0$  for  $T > 0.00025$  and so singularity  $T = 0$  is located inside of trapped surfaces. Thus singularity become invisible from point of view of distant observers.

**Figure 12.** Here  $\Theta_{11}^* > 0$  for  $0 < T < 0.882$  and  $T \geq 1.097$  while it takes negative values for  $0.882 < T < 1.097$ . Singularity is  $T = 0$  and so it become invisible from distant observers.

**Figure 13.** Here  $\Theta_{12}^* > 0$  for  $0 < T < 1.065$  and  $T \geq 1.148$  while it takes negative values for  $1.065 < T < 1.148$ . Singularity is  $T = 0$  and so it become invisible from distant observers.

Table 1. Characteristics of metric parameters

$P_i$	$\mu_i$	$\omega_i$	$(A/B)_i$	$(E/B)_i$	$R_i^*$	$K_i^*$
$P_1$	+2.433	-0.719	+1.450	+1.019	-25.619	+210.786
$P_2$	+2.057	+0.968	+0.029	-0.015	+6.392	+13.345
$P_3$	+1.888	-0.607	-0.174	-0.188	+9.583	+14.424
$P_4$	+1.616	-1.648	+1.633	+1.568	-25.774	+199.272
$P_5$	+0.644	-0.086	-0.001	+0.295	-0.531	+6.690
$P_6$	+0.521	+1.883	+1.478	-4.782	+18.432	+1875.170
$P_7$	+0.508	-1.713	-0.304	+1.086	-3.257	+92.697
$P_8$	-0.041	+3.285	-0.028	-0.009	-0.002	+0.039
$P_9$	-0.201	+0.850	+0.389	-0.672	+0.076	+20.787
$P_{10}$	-0.270	-1.986	-0.044	-0.047	-0.083	+0.269
$P_{11}$	-3.284	-2.013	+3.467	-1.339	+37.305	+456.394
$P_{12}$	-6.206	+0.645	-9.146	-2.433	+68.973	+21412.731

Table 2. Fluid characteristics of stellar cloud.

$P_i$	$\rho_i^*$	$p_{i_r}^*$	$p_{i_t}^*$	$p_i^*$	$\Delta_i(t)$
$P_1$	+3.049	-7.033	-5.452	-7.298	+1.069
$P_2$	+0.925	+0.230	-2.038	-1.317	-0.616
$P_3$	+0.633	+1.061	-1.435	-0.498	-1.198
$P_4$	+3.468	-6.456	-3.300	-5.253	+1.081
$P_5$	+1.486	-0.799	-0.364	-0.410	+0.207
$P_6$	-7.755	+13.316	+2.145	+3.525	+1.117
$P_7$	+2.942	-2.928	-0.622	-0.876	+0.695
$P_8$	+1.037	-0.036	-0.0001	+0.0002	-8.917
$P_9$	+0.074	+0.740	-0.113	-0.157	+0.157
$P_{10}$	+1.010	-0.007	-0.035	-0.031	-0.527
$P_{11}$	+0.590	-0.936	-6.065	-2.162	-0.753
$P_{12}$	+22.814	+113.561	+48.430	+53.458	-7.776

Table 3. Time and radius of formed event and apparent horizons

$P_i$	$T_{EH}/\sqrt{\alpha}$	$T_{AH}/\sqrt{\alpha}$	$R_{EH}/\sqrt{\alpha}$	$R_{AH}/\sqrt{\alpha}$
$P_1$	-	-	-	-
$P_2$	-	+5.453	-	+3.889
$P_3$	+2.526	+1.707	+2.752	+1.188
$P_4$	-	-	-	-
$P_5$	36692.907	-	+38236.634	-
$P_6$	-	+0.032	-	+0.015
$P_7$	+10.427	-	+3.054	-
$P_8$	$1.372 \times 10^{-38}$	-	$1.342 \times 10^{-38}$	-
$P_9$	-	0.082	-	-
$P_{10}$	$9.473 \times 10^{-6}$	$7.099 \times 10^{-6}$	$+9.677 \times 10^{-6}$	-
$P_{11}$	-	-	-	-
$P_{12}$	+1.429	-	+2.647	-

Table 4. Nakedness, trapped surfaces and phase of fluid

$P_i$	$\gamma_i(t)$	Trapped S.	Phase of fluid	Nakedness
$P_1$	-0.669	Full	Domain walls	Covered
$P_2$	-0.323	Quasi	Cosmic sting	Naked
$P_3$	-0.174	Full	Dark matter	Covered
$P_4$	-0.796	No	Domain walls	Naked
$P_5$	-0.563	No	Domain walls	Naked
$P_6$	-0.822	Quasi	Anti-matter	Covered
$P_7$	-0.704	No	Domain walls	Naked
$P_8$	+1.092	No	Stiff matter	Naked
$P_9$	-0.691	Quasi	Domain walls	Covered
$P_{10}$	-0.438	Quasi	Quasi-cosmic string	Covered
$P_{11}$	-0.178	Quasi	Dark matter	Covered
$P_{12}$	-0.552	Quasi	Quasi-domain walls	Covered

Table 5. Numerical values of the black hole formation condition  $\sigma_i \geq 0$

$P_i$	$\sigma_i$
$P_1$	-0.286
$P_2$	-1.490
$P_3$	+0.120
$P_4$	+0.026
$P_5$	-295.830
$P_6$	-4.073
$P_7$	-4.411
$P_8$	-0.700
$P_9$	-2.835
$P_{10}$	-0.076
$P_{11}$	-
$P_{12}$	-

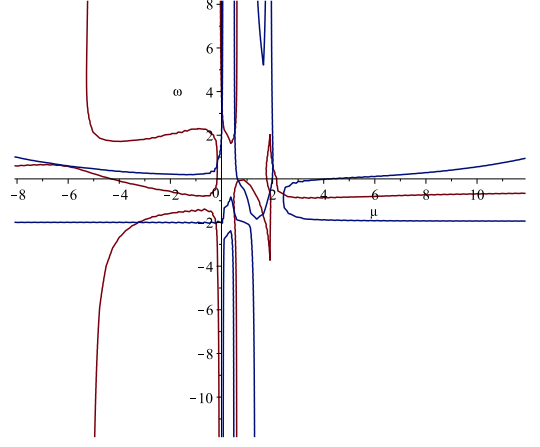


FIG. 1: Diagram of the equations (42) and (44) are plotted against  $(\mu, \omega)$ . Numerical values of crossing points  $P_i \equiv (\mu_i, \omega_i)$  with  $i = 1, 2, 3, 4, \dots, 12$  are given in table 1.

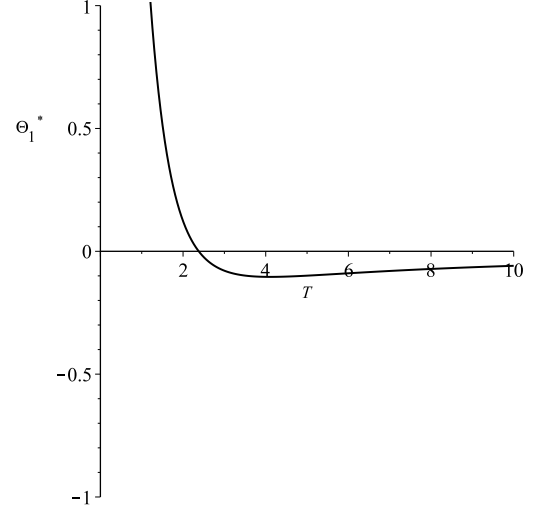
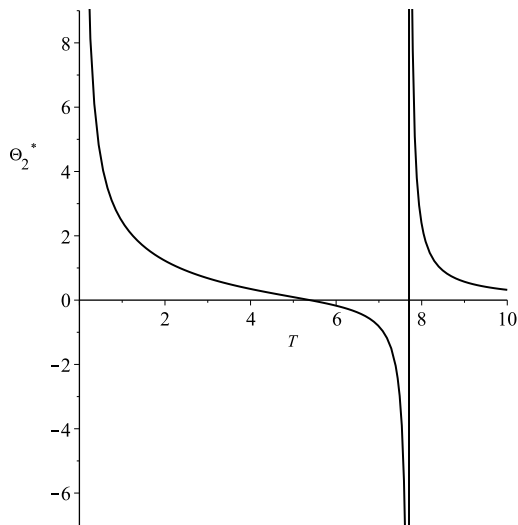
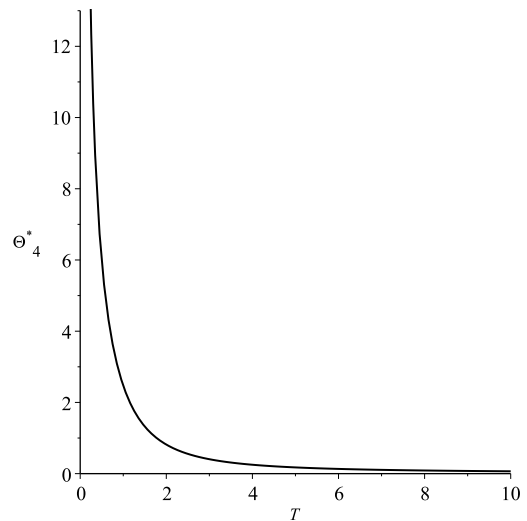
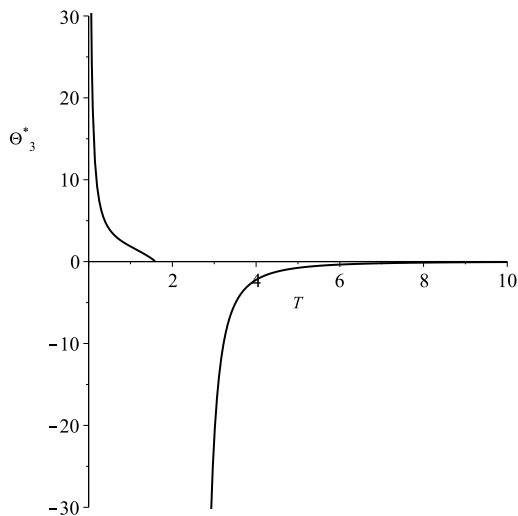
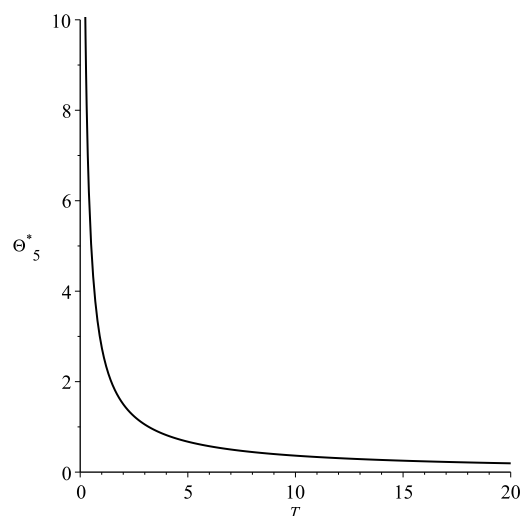


FIG. 2: Diagram of the equation (85) is plotted against  $T$ .

## VI. CONCLUDING REMARKS

We apply an alternative higher order derivative gravity model to obtain time-dependent internal metric solution of an anisotropic spherically symmetric collapsing cloud. We obtain class of solutions (12 different kinds) where geometrical source treats as domain walls (6 kinds), cosmic string (2 kinds), dark matter (2 kinds), stiff matter (1 kind) and anti-matter (negative energy density) with 1 kinds. In summary 7 kinds of our solutions reach to compact object with covered singularity (the black hole) but 5 solutions reach to naked singular metric at end of the collapse and hence cosmic censorship conjecture maintain valid for 7 kinds of our 12 metric solutions only.

FIG. 3: Diagram of the equation (86) is plotted against  $T$ .FIG. 5: Diagram of the equation (88) is plotted against  $T$ .FIG. 4: Diagram of the equation (87) is plotted against  $T$ .FIG. 6: Diagram of the equation (89) is plotted against  $T$ .

## REFERENCES

- 1 D. Lovelock. *Aequationes Mathematicae*, 4(1-2),127, 138, (1970), doi:10.1007/BF01817753.
- 2 D. Lovelock. *J. of Math. Phys.*, 12(3),498,501 (1971), doi:10.1063/1.1665613.
- 3 N. D. Birrell and P. C. W. Davies, *Quantum Fields in Curved space* (Cambridge, England, 1982).
- 4 N. Straumann, *General Relativity*, (Springer-Verlag Berlin Heidelberg 2004).
- 5 B. Fauser, J. Tolksdorf and E. Zeidler *Quantum Gravity* "Mathematical Models and Experimental Bounds", ( Birkhäuser Verlag, P.O.Box 133, CH-4010 Basel, Switzerland, 2007).
- 6 A. A. Starobinsky, *Phys. Let. B*16, 953 (1980).
- 7 V. Müller, H. J. Schmidt and A. A. Starobinsky, *Phys. Let. B*202, 198 (1988).
- 8 S. W. Hawking and J. C. Luttrell, *Nucl. Phys. B*247, 250 (1984).
- 9 U. Kasper, *Class. Quantum Grav.* 10, 869 (1993).
- 10 L. O. Pimentel and O. Obregón, *Class. Quantum Grav.* 11, 2219 (1994).
- 11 H. Elst van, J. E. Lidsey and R. Tavakol, *Class. Quantum Grav.* 11, 2483 (1994).
- 12 W. H. Zurek and D. N. Page, *Phys. Rev. D*29, N4, 628 (1984).

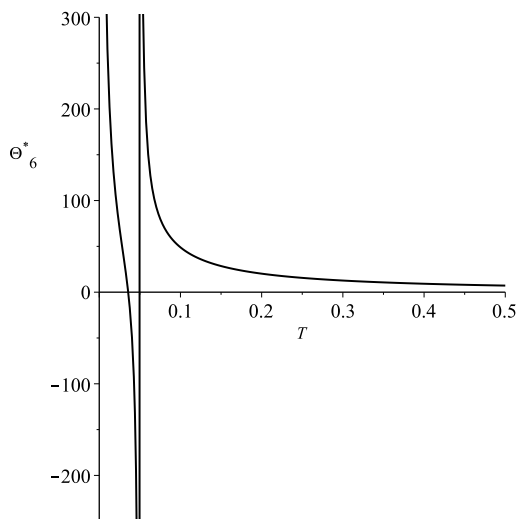


FIG. 7: Diagram of the equation (90) is plotted against  $T$ .

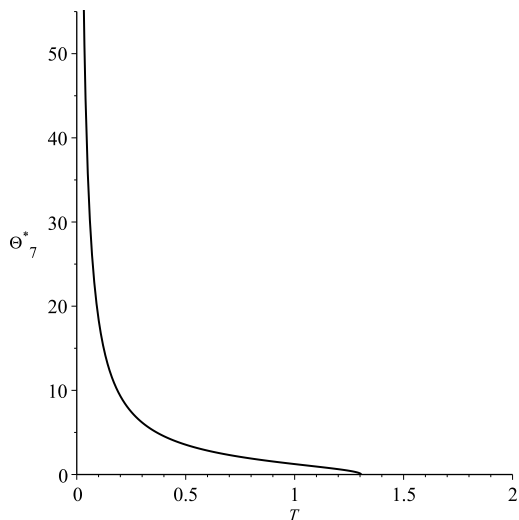


FIG. 8: Diagram of the equation (91) is plotted against  $T$ .

- 13** P. Coles and F. Lucchin, *COSMOLOGY, The origin and evolution of cosmic Structure*, (John Wiley & Sons 1997).
- 14** E. M. Lifshits and L. D. Landau, *The classical theory of fields*, (Pergamon press Ltd, fourth edition 1975).
- 15** S. Weinberg, *Gravitation and Cosmology*, (John Wiley & Sons, Inc, 1972).
- 16** P. Musgrave and K. Lake, *Class. Quant. Grav.* 13 (1996) 1885-1900, gr-qc/9510052v3.
- 17** C. Grenon and K. Lake, *Phys. Rev. D* 84, 083506 (2011), gr-qc/1108.6320.

- 18** R. Doran, F. S. N. Lobo and P. Crawford, *Found. Phys.* 38, 160 (2008), gr-qc/0609042.

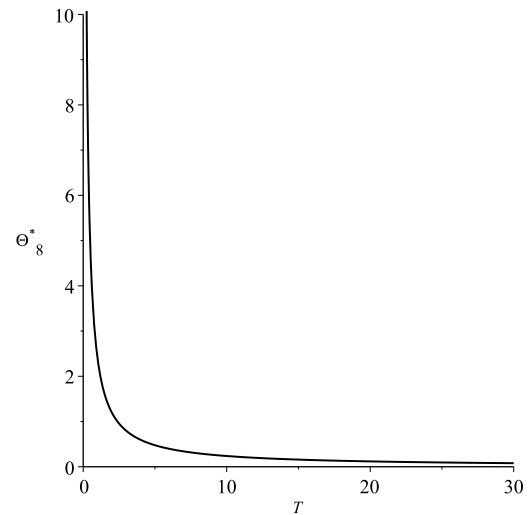


FIG. 9: Diagram of the equation (92) is plotted against  $T$ .

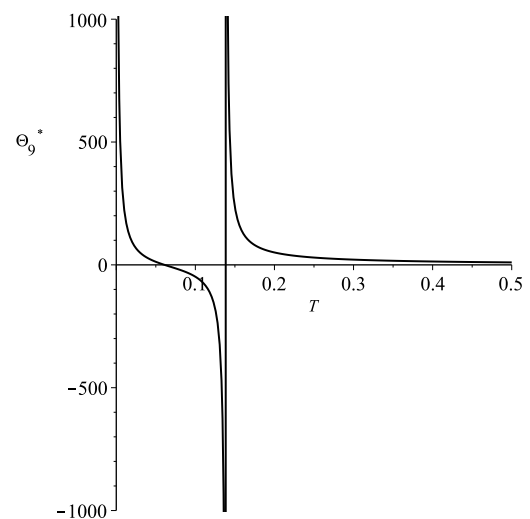


FIG. 10: Diagram of the equation (93) is plotted against  $T$ .

- 19** S. W. Hawking and G. F. R. Ellis, *The large scale structure of space time*, (Cambridge University Press, Cambridge, England, 1973).
- 20** T. Harada, H. Iguchi and L. I. Nakao, gr-qc/0204008 (2002)
- 21** C. W. Misner and D. H. Sharp, *Phys. Rev.* 136, 571 (1964).

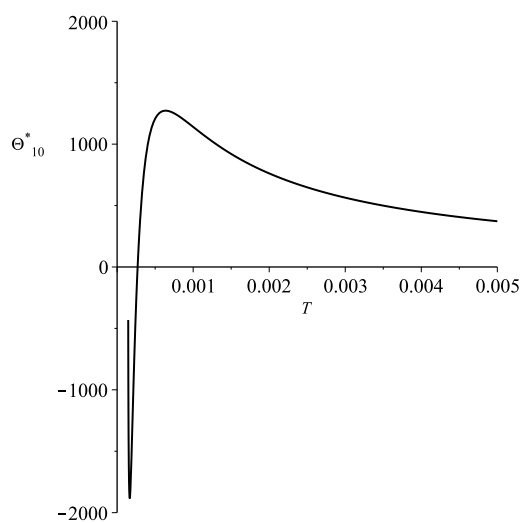


FIG. 11: Diagram of the equation (94) is plotted against  $T$ .

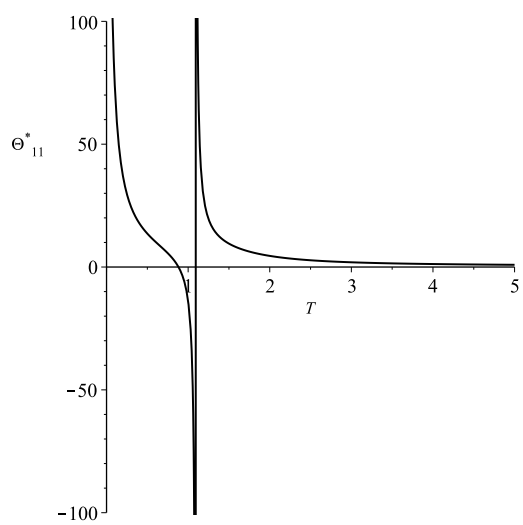


FIG. 12: Diagram of the equation (95) is plotted against  $T$ .

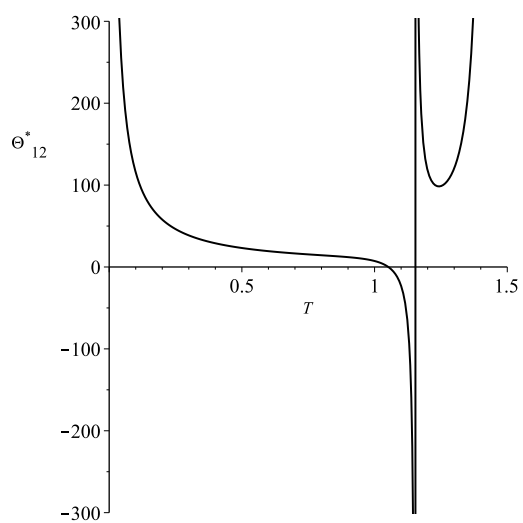


FIG. 13: Diagram of the equation (96) is plotted against  $T$ .